

Rearrangement and Hydrogen Scrambling Pathways of the Toluene Radical Cation: A Computational Study

Daniel Norberg,[†] Per-Erik Larsson,[‡] and Nessima Salhi-Benachou*[†]

Department of Quantum Chemistry, Uppsala University, Box 518, 751 20 Uppsala, Sweden, and SINTEF Materials and Chemistry, N-7465 Trondheim, Norway

Received: November 25, 2007; Revised Manuscript Received: February 29, 2008

A computational study is undertaken to provide a unified picture for various rearrangement reactions and hydrogen scrambling pathways of the toluene radical cation (**1**). The geometries are optimized with the BHandHLYP density functional, and the energies are computed with the ab initio CCSD(T) method, in conjunction with the 6-311+G(d,p) basis set. In particular, four channels have been located, which may account for hydrogen scrambling, as they are found to have overall barriers lower than the observed threshold for hydrogen dissociation. These are a stepwise norcaradiene walk involved in the Hoffman mechanism, a rearrangement of **1** to the methylenecyclohexadiene radical cation (**5**) by successive [1,2]-H shifts via isotoluene radical cations, a series of [1,2]-H shifts in the cycloheptatriene radical cation (**4**), and a concerted norcaradiene walk. In addition, we have also investigated other pathways such as the suggested Dewar–Landman mechanism, which proceeds through **5**, via two consecutive [1,2]-H shifts. This pathway is, however, found to be inactive as it involves too high reaction barriers. Moreover, a novel rearrangement pathway that connects **5** to the norcaradiene radical cation (**3**) has also been located in this work.

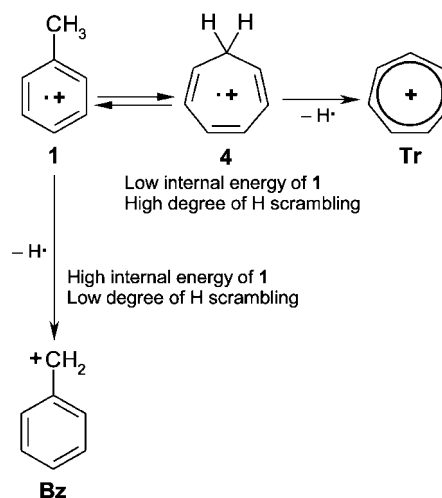
Introduction

The formation of $C_7H_7^+$ from the molecular ion of toluene (**1**) has been the subject of extensive research for the past half-century.¹ It is well-known that tropylium (Tr) and benzylium (Bz) are major $C_7H_7^+$ products upon hydrogen dissociation from **1**, where Tr dominates at low internal energies of **1** while the abundance of Bz increases with increasing energy.^{2,3} It is generally assumed that Bz is formed from **1** by direct C–H bond cleavage while, as suggested by Meyer and Harrison,⁴ Tr is formed by hydrogen loss from the cycloheptatriene radical cation (**4**), as depicted in Scheme 1. The activation energies for these processes have been measured and have been found to be 50.3 kcal/mol⁵ for Tr and 48.7 kcal/mol⁶ for Bz, results that are consistent with recent high-level ab initio computations,⁷ of 51.6 and 49.5 kcal/mol, for Tr and Bz, respectively.

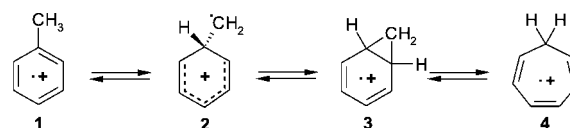
From deuterium labeling studies,^{8,9} it is also known that complete, or nearly complete, hydrogen scrambling accompanies the formation of Tr while the degree of scrambling is reduced¹⁰ when Bz is formed (see Scheme 1). In 1974, Hoffman¹¹ suggested a unified decomposition mechanism for reactions between **1** and **4**. Accordingly, the two compounds are interconvertible by a stepwise skeletal rearrangement mechanism, as depicted in Scheme 2.

First, a methyl hydrogen atom in **1** migrates to the *ipso*-position on the ring, creating a distonic intermediate (**2**). Then, ring closure to the norcaradiene (NCD) radical cation (**3**) followed by ring expansion account for the final transformation to **4** (Scheme 2). Scrambling of all hydrogen atoms in the system can, in terms of the elementary steps in the Hoffman mechanism, occur either by successive interconversions between **1** and **3** with subsequent [1,5]-sigmatropic rearrangement of the CH_2

SCHEME 1: Mechanisms for the Formation of Bz and Tr from 1



SCHEME 2: Hoffman Mechanism for the Rearrangement of 1 to 4



group or by rearrangement to **4** followed by H shifts in the ring. In the [1,5]-sigmatropic rearrangement in **3**, which is commonly referred to as the NCD walk on the neutral potential energy surface (PES), the methylene group circumambulates on the largest ring of NCD.¹²

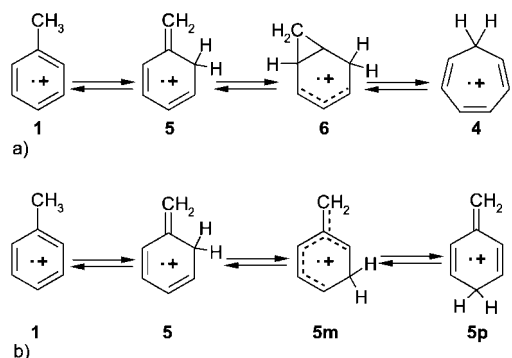
An alternative pathway for the isomerization of **1** to **4** is the Dewar–Landman mechanism,¹³ which was proposed in 1977. This is represented in Scheme 3a where the methyl hydrogen

* To whom correspondence should be addressed. E-mail: Nessima.Salhi@kvac.uu.se.

[†] Uppsala University.

[‡] SINTEF Materials and Chemistry.

SCHEME 3: (a) Dewar–Landman Mechanism for the Rearrangement of 1 to 4 and (b) Complete Hydrogen Scrambling via Isotoluene Radical Cations



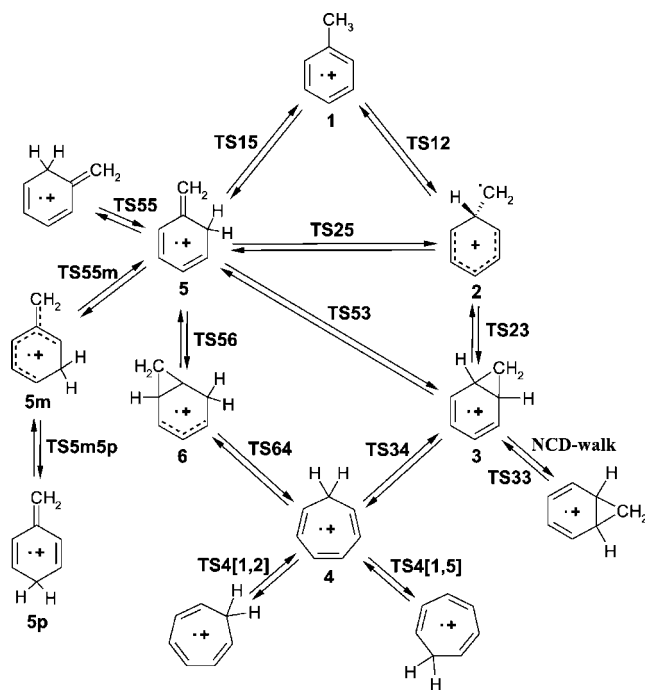
in **1** migrates to the *ortho*-position, yielding the methylenecyclohexadiene radical cation (**5**). This is followed by an intramolecular cyclization of **5** to **6** and eventually by ring expansion and H shift, leading to **4** (Scheme 3a). In addition, another mechanism, which could account for complete hydrogen scrambling, has recently been optimized.⁷ This path is described in Scheme 3b, where **1** first rearranges to **5** and further to the radical cations of *meta*-isotoluene (**5m**) and *para*-isotoluene (**5p**) by successive [1,2]-H shifts.

In a computational investigation, the Hoffman mechanism and the Dewar–Landman pathway were compared at the semiempirical MINDO/3 level.¹³ The two channels were found to be competitive, with overall activation energies of 34.2 and 33.5 kcal/mol for the former and the latter pathways. The rate-determining step for the Hoffman mechanism is found to be the [1,2]-H shift to **2** (Scheme 2), while the step of highest energy in the Dewar–Landman pathway was the concerted [1,3]-H shift from **1** to **5** (Scheme 3a). Moreover, activation energies of 13.9 and 54.9 kcal/mol were found for the [1,2]- and the [1,5]-H shifts in **4**, respectively.¹³ Hence, as **4** was found to lie 5.6 kcal/mol below **1**, these calculations¹³ indicate that the lowest energy pathway for complete hydrogen scrambling in the system was the rearrangement of **1** to **4** by the Dewar–Landman mechanism, followed by [1,2]-H shifts in **4**. In addition, these computations¹³ suggested that complete carbon scrambling should proceed as easily as complete hydrogen scrambling. In 1993, Lifshitz et al.¹⁴ conducted the first ab initio investigation on the rearrangement of **1** to **4** with the purpose of modeling the [Tr]/[Bz] ratio as a function of the internal energy of **1**. Hence, using the Hartree–Fock (HF) method for geometry optimization and a combined approach with several post-HF levels in conjunction with the small 3-21G basis set for computing the energies, the authors computed the PESs for the Hoffman mechanism and the Dewar–Landman pathway. Only the Hoffman channel was found to be significant in this study,¹⁴ while the Dewar–Landman pathway was discarded as it was reported to involve too high barriers. Again, the [1,2]-H shift to **2** was predicted to be rate-determining, but the computed activation energy, 45 kcal/mol, suggested that the barrier heights calculated in the earlier MINDO/3 study were severely underestimated. Moreover, Lifshitz et al. computed¹⁴ an energy difference of 17 kcal/mol between **4** and **1**, which was consistent with the experimental¹⁵ relative heat of formation at 0 K of 18.5 kcal/mol. These results cast doubts on the reliability of the MINDO/3 results. Unfortunately, because the objective of Lifshitz and her co-workers¹⁴ was not to investigate different routes for hydrogen scrambling, no computations were performed on the [1,2]- nor on the [1,5]-H shifts in **4**.

With the purpose of modeling the effects of substitution on the rearrangement of **1**, the Hoffman mechanism was reinvestigated by Grützmacher and Harting in 2003.¹⁶ Geometries and energies were calculated with HF and with the B3LYP functional of density functional theory (DFT) in conjunction with the 6-311+G(3df,2p) basis set. However, these two methods predicted widely different activation energies for the rate-determining step: 45.8 and 36.9 kcal/mol with HF and B3LYP, respectively.¹⁶ Moreover, in the B3LYP calculations, **2** was found to correspond to a transition state (TS) between **1** and **3**, indicating that this species was not stable. In 2006, this peculiar issue was addressed by Choe⁷ who applied the high-level G3//B3LYP method [B3LYP/6-311++G(d,p) for geometries and G3//B3LYP/6-31G(d) for the energies] on the Hoffman mechanism. Thus, in this study,⁷ **2** was found to be a stable species at the B3LYP level. In addition, the [1,2]-H shift to **2** was once again predicted to be rate-determining, with an activation energy of 38.0 kcal/mol at the G3//B3LYP level, which was lower than the ab initio barrier height of Lifshitz et al.¹⁴ Again, with the purpose of modeling the [Tr]/[Bz] ratio, Choe also investigated the rearrangement of **1** to the isotoluene structures (Scheme 3b). However, in contradiction to the MINDO/3 study,¹³ this author found a pathway for the initial transformation of **1** to **5**, which proceeds through **2**, while the concerted [1,3]-H shift was not addressed in this last study.⁷ Interestingly, it was found that the [1,2]-H shift to **2** was the rate-determining step also for the total isomerization of **1** to **5p**. This result suggested that **1** underwent hydrogen scrambling via isotoluene structures as easily as it rearranged to **4** by the Hoffman mechanism.

Despite the wealth of both experimental and theoretical information about the toluene molecular ion rearrangement, which is available in the literature, a unified understanding of the most probable pathways for the hydrogen scrambling processes is missing. Furthermore, there are a number of aspects that remain unclear or that have not been fully taken into account. First, the importance of the Dewar–Landman mechanism in the **1**–**4** rearrangement has not been properly established. This is supported by the relatively large difference in activation energy between the ab initio approach of Lifshitz and co-workers¹⁴ and the G3//B3LYP computations of Choe⁷ for the Hoffman mechanism. Second, because the [1,2]- and [1,5]-H shifts in **4** have, to the best of our knowledge, only been investigated¹³ at the MINDO/3 level, yielding energies of doubtful quality, a renewed study of these reactions, at higher levels of calculation, is strongly motivated. Third, the NCD walk could be of great importance for the understanding of the scrambling pathways in the system. However, in the earlier study of Grützmacher and Harting,¹⁶ this process was found to occur through different routes at the HF and B3LYP levels of computation. On the one hand,¹⁶ a stepwise pathway was predicted with HF, while **2** was found to be unstable with B3LYP, as mentioned above. On the other hand,¹⁶ a concerted mechanism was located with B3LYP but not with HF. Therefore, to elucidate the mechanisms of the scrambling pathways in this system, we have reinvestigated both the Hoffman mechanism and the Dewar–Landman pathway in the present work. In addition, we have also investigated in detail the NCD walk as well as the [1,2]- and [1,5]-H shift processes in **4**. Finally, the routes for hydrogen scrambling via isotoluene radical cations have also been addressed. All channels investigated in the present study are introduced in Scheme 4 together with all located stationary points.

SCHEME 4



Computational Details

The Gaussian03 suite of programs¹⁷ has been used for the quantum chemical calculations presented in this work, and all of the abbreviations are taken from this program package. Molekel¹⁸ has been used for the inspection of final geometries and vibrational frequencies and for making pictures of the optimized stationary points.

All computations have been performed in the unrestricted formalism and in conjunction with the 6-311+G(d,p) basis set, unless otherwise indicated. The geometries of the stationary points have been optimized with the BHandHLYP hybrid DFT method, without any symmetry constraint and using default convergence criteria on both nuclear displacements and forces. Electronic energies of the BHandHLYP optimized structures have been computed with the coupled-cluster CCSD(T) method, within the frozen core approximation, using a convergence criterion of 10^{-10} on the root-mean-square of the SCF density matrix. The CCSD(T) energies and the unscaled BHandHLYP frequencies have been employed to calculate corrections to the Gibbs free energy and the thermal heat of formation at 298.15 K and 1.0 atm. The imaginary normal mode vector of each TS has been analyzed to make sure that it represents the correct distortion of the nuclear framework, leading to reactant and product. Also, the intrinsic reaction coordinate (IRC) algorithm has been used to follow the minimum energy paths (MEPs) downhill from each saddle point in the skeletal rearrangement paths. Unless otherwise indicated, the Gibbs free energies are used in the discussion.

An attempt was first made to perform the present study with the popular B3LYP functional of DFT, which would have allowed for a consistent comparison with the results of Choe.⁷ However, not all of the transition structures of the Dewar–Landman pathway could be located at this level. We also tried to use the MP2 method, which, on the other hand, was found to suffer from high spin contamination for most of the stationary points ($\langle S^2 \rangle$ between 0.766 and 1.144). Furthermore, the MP2 geometry optimization of the toluene molecular ion yielded an asymmetric structure, which resulted in electron spin resonance

TABLE 1: CCSD(T) Computed Energies (in kcal/mol) of the Stationary Points in the Hoffman Mechanism^a

	absolute			relative		
	BHandHLYP	B3LYP	Δ_{abs}	BHandHLYP	B3LYP	Δ_{rel}
1	-169776.16	-169777.49	1.3	0.0	0.0	0.0
TS12	-169735.99	-169737.23	1.2	40.2	40.3	-0.1
2	-169741.28	-169742.30	1.0	34.9	35.2	-0.3
TS23	-169740.55	-169741.94	1.4	35.6	35.6	0.0
3	-169758.79	-169760.20	1.4	17.4	17.3	0.1
TS34	-169749.48	-169750.66	1.2	26.7	26.8	-0.1
4	-169758.90	-169760.20	1.3	17.3	17.3	0.0

^a The geometry optimization was performed with BHandHLYP and B3LYP (see text). The 6-311+G(d,p) basis set was used in all of the calculations. Δ_{abs} (Δ_{rel}) is the difference between the absolute (relative) energies computed with CCSD(T)//BHandHLYP and CCSD(T)//B3LYP.

(ESR) parameters deviating substantially from the observed ones. Therefore, we decided to use the BHandHLYP functional of DFT for the geometry optimization calculations. To further justify the use of BHandHLYP in the present study, we undertook a computational evaluation of the performances of BHandHLYP and B3LYP in the Hoffman mechanism (see Scheme 2), where all of the stationary points could be optimized with both methods. In this side study, minor deviations were found between the BHandHLYP/6-311+G(d,p) and the B3LYP/6-311+G(d,p) geometries. For each stationary point, the energy was calculated with CCSD(T) on the geometries obtained with both DFT methods. As shown in Table 1, all of the absolute CCSD(T)//BHandHLYP energies were found to be larger than those computed at the CCSD(T)//B3LYP level, the largest deviation being 1.4 kcal/mol. Yet, the most important result of this side study is that the relative energies calculated at the two levels were found to be essentially the same, the largest deviation being 0.3 kcal/mol.

Results and Discussion

Three channels for the skeletal rearrangement of **1** to **4** have been located in the present work. The first pathway, **1**–**TS12**–**2**–**TS23**–**3**–**TS34**–**4**, corresponds to the Hoffman mechanism (see Scheme 4). Both the second and the third pathways from **1** to **4** involve initial isomerization to **5**, a process that in turn may proceed by a concerted [1,3]-H shift or through a stepwise mechanism via **2**. The continued rearrangement from **5** to **4** proceeds either by the Dewar–Landman mechanism, **5**–**TS56**–**6**–**TS64**–**4**, or via the route, **5**–**TS53**–**3**–**TS34**–**4**, where **TS53** connects the methylenecyclohexadiene radical cation with NCD. In addition, we have located two TSs of importance for the NCD walk, **TS22** and **TS33**, where **TS22** corresponds to internal rotation of the methylene group in **2** and **TS33** connects two **3** isomers by a concerted [1,5]-sigmatropic rearrangement (concerted NCD walk). Moreover, the TSs for the [1,2]- and [1,5]-H shifts in **4**, **TS4[1,2]**, and **TS4[1,5]**, respectively, as well as the stationary points involved in complete hydrogen scrambling via isotoluene radical cation structures, **5**–**TS55m**–**5m**–**TS5m5p**–**5p**, have been located. Finally, another path, where the two methylene groups in **5** are exchanged and which proceeds via **TS55**, has also been studied.

The BHandHLYP-optimized minima **1**–**4**, involved in the Hoffman mechanism, are displayed in Figure 1, with selected geometrical parameters, while the optimized minima **5** and **6** involved in the Dewar–Landman pathway, as well as the isotoluene radical cation species **5m** and **5p**, are displayed in Figure 2.

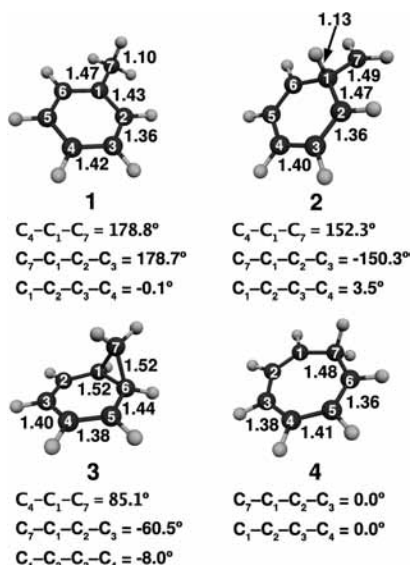


Figure 1. BHandHLYP/6-311+G(d,p) optimized structures of the minima involved in the skeletal rearrangement of **1** to **4** by the Hoffman mechanism. Bond lengths are in Ångströms.

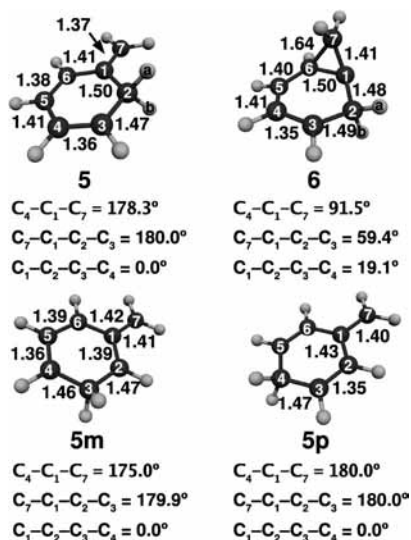


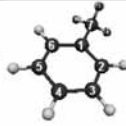
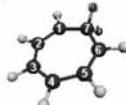
Figure 2. BHandHLYP/6-311+G(d,p) optimized structures of the minima involved in the skeletal rearrangement of **1** to **4** by the Dewar-Landman mechanism, as well as the optimized structures of the *meta*- and *para*-isotoluene radical cations. Bond lengths are in Ångströms.

A comparison of the **1**–**5m,5p** structures in Figures 1 and 2, with the corresponding geometries optimized by Choe⁷ at the B3LYP/6-311++G(d,p) level, reveals that BHandHLYP predicts bond lengths that are systematically shorter, with an average (maximum) deviation of -0.01 Å (-0.02 Å) from B3LYP. Despite this systematic discrepancy, the two methods are found to predict similar geometries of the minima. For structure **6**, we note that the C_6-C_7 bond is found to be 0.07 Å longer with BHandHLYP than the value of 1.57 Å predicted¹³ with MINDO/3.

The hyperfine coupling constants (hfcc's) computed with BHandHLYP for the protons in **1** and **4** are displayed in Table 2 together with available experimental ESR parameters. It is noted from this table that the calculated hfcc for the hydrogen at the *para*-position of **1**, -12.4 G, is in excellent agreement with the corresponding experimental result. Because of a low barrier for methyl rotation in **1**,¹⁹ the calculated hfcc's in the methyl group have to be averaged to reflect the experimental conditions. As can be seen in Table 2, such a calculated mean value (19.4 G) becomes very close to the experimental values (18.5^{20} and 19.0^{21} G). For compound **4**, a good agreement is found between the observed²² and the computed ESR parameters of all but the H1 and the H6 protons, as can be seen in the table. This analysis validates the use of BHandHLYP method to compute hfcc's.²³ Also, it is known that the ability of a computational method to reproduce the observed ESR spectra provides a strong indication for a high quality of the optimized structure. Hence, the results presented in Table 2 show that BHandHLYP is a good method for geometry calculations in these systems.

The BHandHLYP-optimized TSs involved in the Hoffman mechanism, **TS12**, **TS23**, and **TS34**, as well as the **TS22**, **TS33**, **TS4[1,2]**, and **TS4[1,5]** structures, are displayed in Figure 3, with selected geometrical parameters. Similarly, the optimized TSs involved in the Dewar-Landman pathway, **TS15**, **TS25**, **TS56**, and **TS64**, as well as the **TS53**, **TS55**, **TS55m**, and **TS5m5p** structures, are displayed in Figure 4. A comparison of the C–C bond lengths in the structures **TS12**, **TS23**, **TS34**, **TS25**, **TS55m**, and **TS5m5p** with the corresponding distances optimized by Choe⁷ at the B3LYP/6-311++G(d,p) level shows that BHandHLYP again predicts bond lengths that are systematically shorter with an average (maximum) deviation of -0.01 Å (-0.03 Å) from the B3LYP bond lengths. The same trend is noted for the distances involved in the breaking and forming bonds in these TSs. In particular, the maximum deviation is found for the C_6-C_7 distance in **TS23**, which is computed to

TABLE 2: BHandHLYP/6-311+G(d,p) Calculated Proton hfcc's (¹H hfcc's), in Gauss, for **1** and **4**

		1									
		$a_{\text{H}(2)}$	$a_{\text{H}(3)}$	$a_{\text{H}(4)}$	$a_{\text{H}(5)}$	$a_{\text{H}(6)}$	$a_{\text{H}(7a)}$	$a_{\text{H}(7b)}$	$a_{\text{H}(7c)}$		
BHandHLYP		-3.2	0.5	-12.4	0.4	-3.1	40.8	8.0	9.3		
Average									19.4		
Exp ^a									18.5		
Exp ^b									19.0		
		4									
		$a_{\text{H}(1)}$	$a_{\text{H}(2)}$	$a_{\text{H}(3)}$	$a_{\text{H}(4)}$	$a_{\text{H}(5)}$	$a_{\text{H}(6)}$	$a_{\text{H}(7a)}$	$a_{\text{H}(7b)}$		
BHandHLYP		-9.4	0.9	-5.5	-5.5	0.9	-9.4	50.0	50.0		
Exp ^c		5.7	–	5.7	5.7	–	5.7	51.5	51.5		

^a ¹H hfcc's assigned to an ESR spectrum of the toluene radical cation in a CFC1₃ matrix at 77 K.²¹ ^b ¹H hfcc's assigned to an ESR spectrum of the toluene radical cation in solid Argon at 16 K.²⁰ ^c ¹H hfcc's assigned to an ESR spectrum of the cycloheptatriene radical cation in a CF₂C1CFCl₂ matrix at 77 K.²²

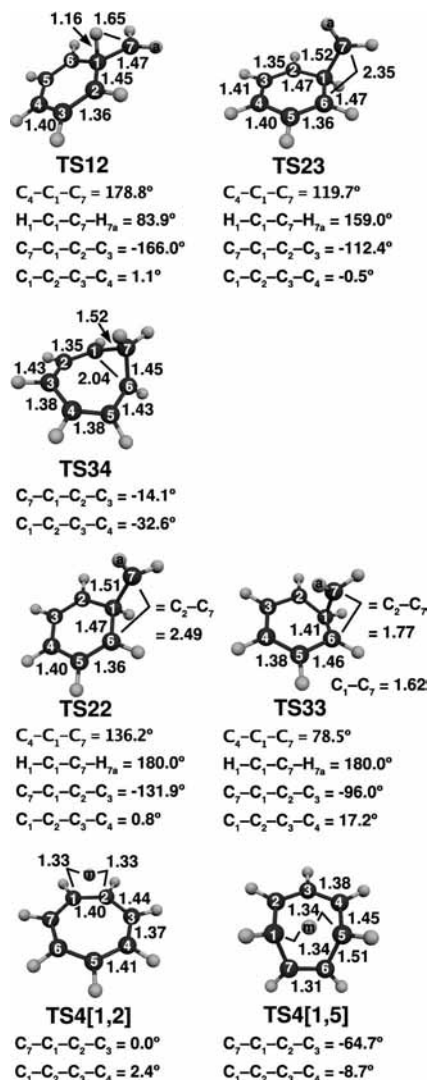


Figure 3. Optimized geometries of the TSs involved in the skeletal rearrangement of **1** to **4** by the Hoffman mechanism: **TS12**, **TS23**, and **TS34**; methylene rotation in **2**: **TS22**; interconversion of two 3 structures: **TS33**; and [1,2]- and [1,5]-H shifts in **4**: **TS4[1,2]** and **TS4[1,5]**, respectively. All calculations were done at the BHandHLYP/6-311+G(d,p) level. Bond lengths are in Ångströms.

be 0.15 Å shorter with BHandHLYP as compared to the same distance optimized⁷ with B3LYP. Thus, on this reaction path, **TS23** is found to be earlier with BHandHLYP than with B3LYP. Otherwise, for the bond-breaking and -forming distances in the other five TSs, the predictions of the two methods do not deviate by more than 0.05 Å. Also, it is noted that BHandHLYP predicts a much later TS than MINDO/3¹³ for the ring closure of **5** to **6**. This is reflected by the fact that the BHandHLYP (MINDO/3¹³) C_6-C_7 distance in **TS56** is 1.70 Å (1.84 Å), which is 0.06 Å (0.27 Å) longer than the corresponding distance in **6**.

Experimentally determined heats of formation are reported¹⁵ for species **1**, **4**, and **5**, which are in good agreement with our CCSD(T)/BHandHLYP calculations. Hence, the heats of formation of **4** and **5** relative to **1**, at 298.15 K, are found to be 18.1 (19.4) and 8.9 (7.9) kcal/mol with the CCSD(T)/BHandHLYP method (experiment¹⁵), respectively. It should also be noted that the relative heat of formation of **4** at 0 K is computed to be 18.5 kcal/mol, which is in close agreement with the experimental¹⁵ value of 19.1 kcal/mol. This is an improvement over the theoretical prediction⁷ using the G3//B3LYP level, which gave a heat of formation of 17.9 kcal/mol.

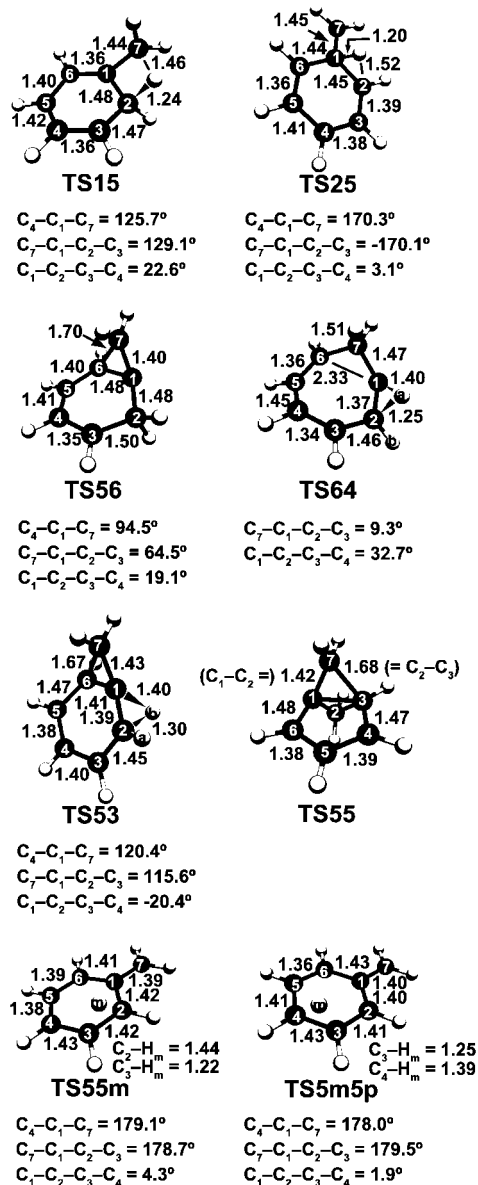


Figure 4. Optimized geometries of the TSs involved in the skeletal rearrangement of **1** to **4** by the Dewar–Landman mechanism.

Hoffmann Mechanism and NCD Walk. A Gibbs energy profile for the isomerization of **1** to **4** by the Hoffman mechanism is displayed in Figure 5. This figure also shows the barriers for internal rotation of the methylene group in **2**, concerted NCD walk, as well as the [1,2]- and [1,5]-H shifts in **4**.

In agreement with the earlier theoretical studies,^{7,13,14,16} it is found that the first step of the Hoffman mechanism, the conversion of **1** to **2**, is rate-determining for this channel. The computed activation energy of 38.7 kcal/mol is very close to the 38.0 kcal/mol barrier predicted in the recent study⁷ with G3//B3LYP. The ring closure to **3**, which is 14.0 kcal/mol more stable than **2**, proceeds with a low activation energy, 1.8 kcal/mol, thereafter followed by ring expansion to **4**, with a barrier of 8.2 kcal/mol. As we previously noted,²⁴ **4** is found to be only slightly more stable than **3** (−0.8 kcal/mol), a result that is also consistent with the recent G3//B3LYP computational study⁷ of Choe.

In Figure 5, it can also be noted that the [1,2]-H shift in **4** proceeds with a much larger activation energy than predicted¹³ with MINDO/3. Thus, the Gibbs barrier height computed here with CCSD(T)/BHandHLYP is found to be 24.2 kcal/mol, and

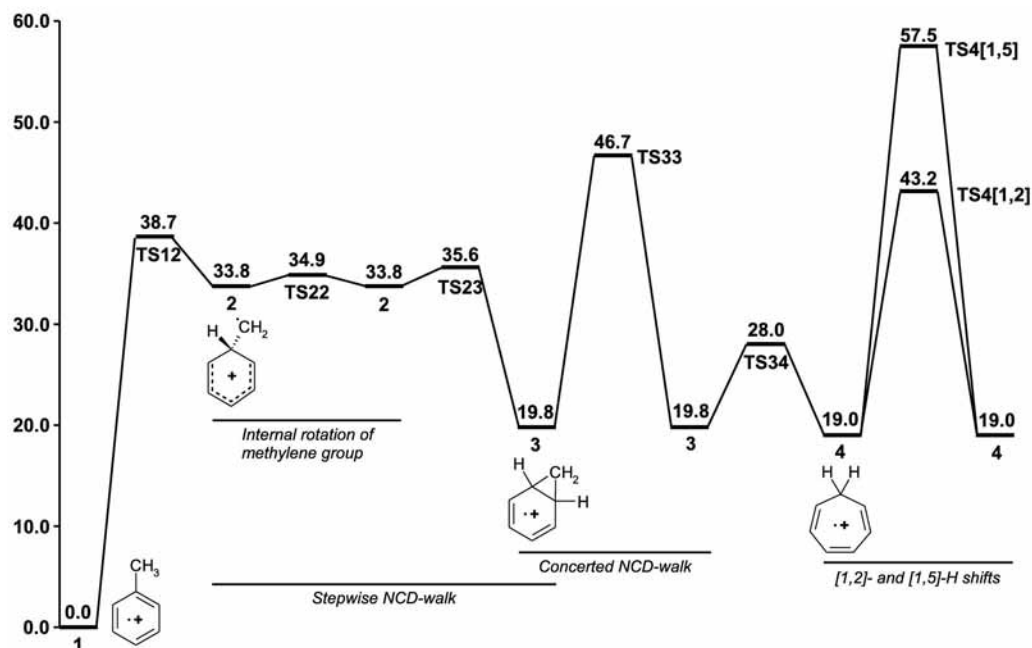


Figure 5. Gibbs energy profiles (in kcal/mol) computed from CCSD(T)/6-311+G(d,p) electronic energies and BHandHLYP/6-311+G(d,p) thermal corrections to Gibbs free energies at 298.15 K and 1.0 atm for the skeletal rearrangement of **1** to **4** by the Hoffman mechanism, the internal rotation of the methylene group in **2**, the concerted NCD walk, and the [1,2]- and [1,5]-H shifts in **4**.

TS4[1,2] lies 4.4 kcal/mol higher than **TS12**. In contrast, MINDO/3 predicted **TS4[1,2]** to lie 26 kcal/mol below **TS12**.¹³ However, with both CCSD(T)//BHandHLYP and MINDO/3, the [1,5]-H shift through **TS4[1,5]** is found to have a barrier that is higher than that of hydrogen loss, which is ~ 50 kcal/mol (Figure 5). Consequently, the hydrogen shifts in **4** are found to have higher activation energies than successive interconversions of **1** and **4** via the Hoffman mechanism with CCSD(T)//BHandHLYP.

For the NCD walk, we located one concerted and one stepwise channel. The stepwise path, **3**–**TS23**–**2**–**TS23**–**3** has an overall activation energy of 15.8 kcal/mol. The internal rotation of the methylene group in the distonic ion **2** has a 0.7 kcal/mol lower activation energy than that of ring closure to **3**. Hence, the stepwise NCD walk on the PES of $C_7H_8^{+\cdot}$ will result in both inversion and retention of the CH_2 configuration. The concerted channel for the NCD walk proceeds through **TS33** with inversion of CH_2 configuration and cannot compete with the stepwise paths because of its much higher barrier of 26.9 kcal/mol. However, the relative energy of **TS33**, 46.7 kcal/mol (see Figure 5), is still below the limit for hydrogen loss, indicating that this path might be activated at energies close to this threshold. Moreover, no concerted channel with retention of CH_2 configuration could be located for the NCD walk. Finally, it should be noted that the radical cation NCD walk is quite different from the corresponding neutral walk. For neutral norbornadiene, Kleiss et al.¹² reported on concerted TSs for both retention and inversion of the CH_2 configuration. At the CASPT2 level of calculation, the activation energies were found¹² to be 44.3 and 44.8 kcal/mol for the corresponding concerted reactions, respectively. Hence, upon ionization, the barrier for the NCD walk drops to less than half of the values predicted for the neutral PESs.

Dewar–Landman Pathway. A Gibbs energy profile for the isomerization of **1** to **4** by the Dewar–Landman pathway is displayed in Figure 6. In addition, this figure also shows the barrier for the concerted rearrangement of **5** to **3**.

The first step in the Dewar–Landman channel is the migration of a hydrogen atom from methyl to *ortho*-position in **1**. This

reaction may proceed stepwise by two consecutive [1,2]-H shifts, **1**–**TS12**–**2**–**TS25**–**5**, or concerted via a [1,3]-H shift, **1**–**TS15**–**5**. As can be noticed from Figure 6, for the stepwise reaction, **TS12** is rate-limiting, while the second step, proceeding through **TS25**, has an activation energy of only 2.4 kcal/mol. On the contrary, the barrier for the concerted hydrogen transfer is found to be 68.7 kcal/mol, which implies that this path is inactive. This high activation energy contrasts with the MINDO/3 barrier of 33.5 kcal/mol.¹³ However, a high activation energy for the [1,3]-H shift is not surprising, since a barrier of 33.2 kcal/mol was computed,²⁵ at the MP4/6-31G(d,p) level, for the more flexible propene radical cation.

The second step in the Dewar–Landman pathway is the ring closure of **5** to **6** (see Figure 6). The computed activation energy for this reaction is 40.3 kcal/mol, which is 11.4 kcal/mol higher than the MINDO/3 result.¹³ In addition, the relative energies of **6** and **TS56** are found to be 50.5 and 50.3 kcal/mol, respectively, which is at the threshold for hydrogen loss, indicating that these species are rare. This result also indicates that **6** is a highly unstable intermediate for the back reaction to **5**, a fact that is reinforced by the late **TS56** with a C_6 – C_7 distance of 1.70 Å as compared to 1.64 for the same distance in **6**.

The last step in the Dewar–Landman pathway (**6** to **4**) is a concerted H shift and ring opening, which has an activation energy of 21.8 kcal/mol. For this reaction step, we located a TS, **TS64**, where H_a is the hydrogen that is being transferred. The IRC calculations reveal a complex reaction coordinate for this transformation. Thus, the uphill path is an asynchronous process where the breaking of C_1 – C_6 dominates the first part of the IRC, while the H_a transfer starts energetically near the TS. Even the downhill path is asynchronous where the first part of the IRC is dominated by continued H_a transfer, whereas the latter part is a combined flattening of the complete structure and continued elongation of the C_1 – C_6 distance. Noteworthy, in the MINDO/3 reported structure¹³ of the corresponding TS, it is H_b that is transferred from C_2 to C_1 (see Figure 4 for the atom labels). All of our attempts to optimize such a TS have failed.

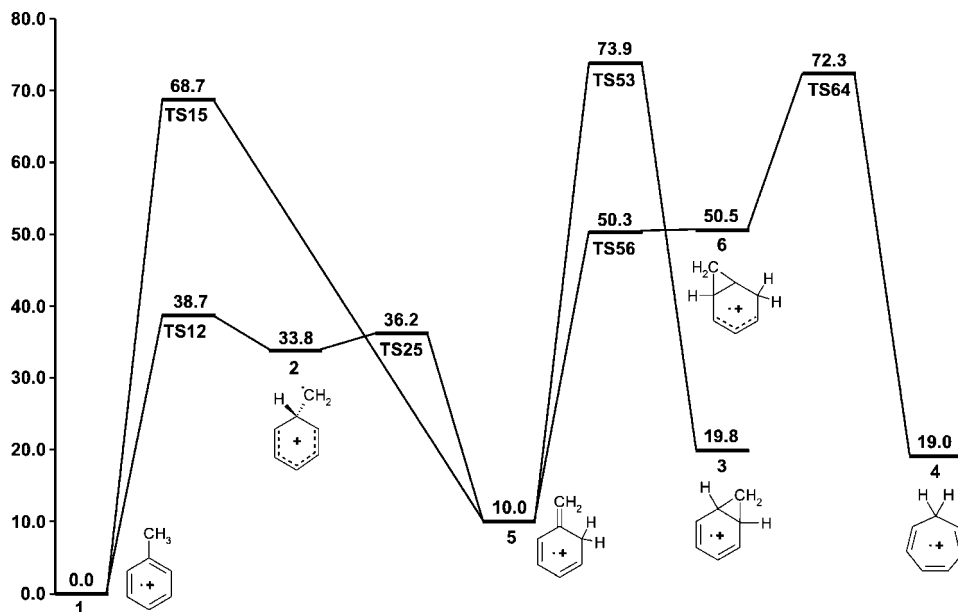


Figure 6. Gibbs energy profile (in kcal/mol) computed from CCSD(T)/6-311+G(d,p) electronic energies and BHandHLYP/6-311+G(d,p) thermal corrections to Gibbs free energies at 298.15 K and 1.0 atm for the skeletal rearrangement of **1** to **4** by the Dewar–Landman pathway and the isomerization of **5** to **3**.

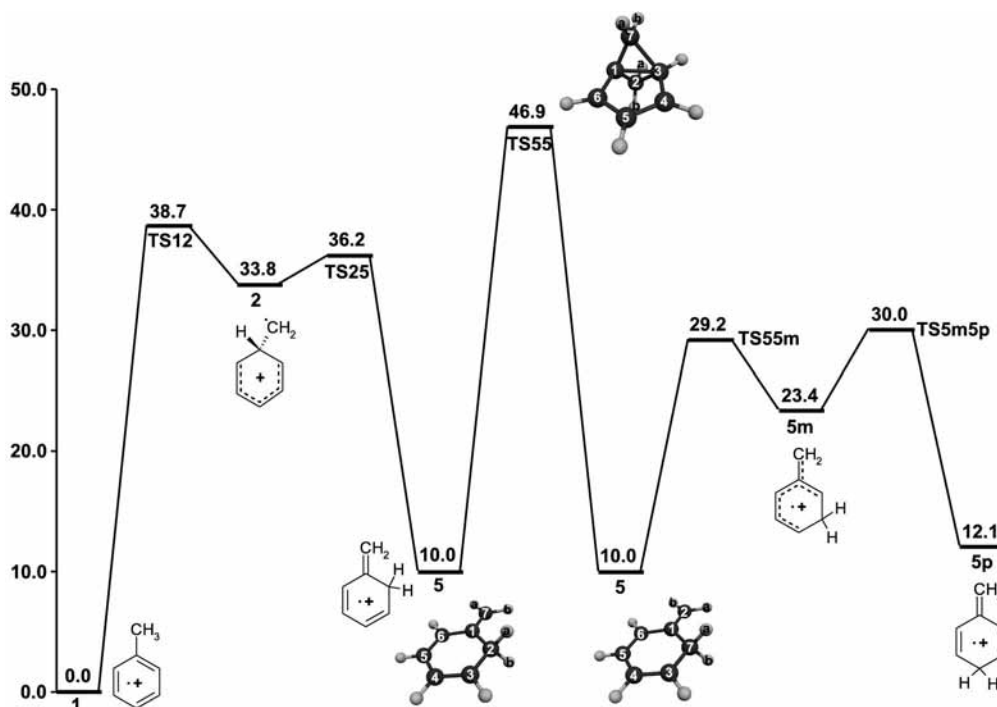


Figure 7. Gibbs energy profile (in kcal/mol) computed from CCSD(T)/6-311+G(d,p) electronic energies and BHandHLYP/6-311+G(d,p) thermal corrections to Gibbs free energies at 298.15 K and 1.0 atm for the isomerization of **1** to **5p** and the exchange of the methylene groups in **5**.

A similar reaction coordinate is noted for the conversion of **5** to **3**, which has a very high barrier of 63.9 kcal/mol, as can be seen in Figure 6. The total reaction, proceeding through **TS53**, is a concerted transfer of the hydrogen H_b from C_2 to C_1 and C_6 – C_7 bond formation (see Figures 1, 2, and 4 for species **3**, **5**, and **TS53**, respectively). Even for this rearrangement, the hydrogen transfer starts energetically near the TS, while the most important geometrical change in the first part of the IRC is the formation of the C_6 – C_7 bond. Finally, by inspection of the geometries of **TS4[1,2]** and **TS4[1,5]** in Figure 3, it can be seen that the former TS has an almost planar carbon skeleton, while the latter is highly bent, a result that is in agreement with the corresponding TSs previously¹³ optimized with MINDO/3. In

summary, all of the paths related to the methylenecyclohexadiene radical cation have substantial barriers; therefore, it can be concluded that the Hoffman mechanism is the lowest energy pathway for isomerization from **1** to **4**.

Isotoluene Radical Cations. In Figure 7, the Gibbs energy profiles for the isomerization of **1** to **5p** and for the exchange of the methylene groups in **5** are displayed. The first (**1**–**2**) and second (**2**–**5**) steps of the **1** to **5p** isomerization have been described above. In the third step, an *ortho*-hydrogen atom is transferred to *meta*-position via **TS55m**, with an activation energy of 19.2 kcal/mol. A relative energy of 23.4 kcal/mol is computed for compound **5m**, which is hence less stable than the other **5** and **5p** isotoluene radical cations. This is consistent with the previous G3//B3LYP results.⁷

The final hydrogen transfer to **5p** is exothermic by 11.3 kcal/mol and proceeds through a barrier of only 6.6 kcal/mol. By comparing the relative energies of the TSs involved in the total rearrangement of **1** to **5p**, it is concluded that the first step is rate-limiting (see Figure 7).

We have also investigated the possibility of methylene exchange in **5** and collected our results in Figure 7, where the carbon atom labels in **5** and **TS55** are used to clarify this transformation. In this figure, it can be seen that, as compared to **5**, extra bonds are formed in **TS55** between C₇ and C₃, on the one hand, and between C₁ and C₃, on the other hand. After **TS55**, both the C₁–C₃ bond and the C₂–C₃ bonds are broken, yielding a complete methylene exchange. It should be noted that the relative energy of **TS55** is predicted to be 46.9 kcal/mol, which is lower than the threshold for hydrogen loss. This result indicates that the methylene exchange will become activated at energies close to this threshold.

Hydrogen Scrambling Pathways. The pathways that may contribute to complete hydrogen scrambling in **1** are required to have overall barriers below the threshold of ~50 kcal/mol for hydrogen dissociation. Four of the located channels fulfill this criterion, and two lowest energy pathways have been found. In one of these, the scrambling proceeds by the stepwise NCD walk involved in the Hoffman mechanism (Figure 5). In the other lowest energy pathway, the hydrogen atoms are scrambled via isotoluene radical cations, and this does not require any skeletal rearrangement (Figure 7). Both of these pathways are limited by the hydrogen transfer from methyl to the *ipso*-position in **1**, with an activation energy of 38.7 kcal/mol. Moreover, scrambling of the hydrogen atoms by [1,2]-H shifts in **4** is found to have a higher barrier (43.2 kcal/mol; see Figure 5). In addition, with an activation energy of 46.7 kcal/mol, the concerted NCD walk of the Hoffman mechanism (Figure 5) also constitutes a possible candidate for hydrogen scrambling. The remaining pathways are all found to have barriers that exceed by far the energy required for hydrogen dissociation.

Our results clearly clarify the role that the NCD walk plays in the complete scrambling of hydrogen atoms in rearrangements from **1**. Moreover, the importance of the **1**–**2** step as the rate-determining step for the scrambling via isotoluene radical cations should also be emphasized.

Conclusions

A quantum chemical investigation has been undertaken to investigate the hydrogen scrambling pathways of the toluene radical cation (**1**). At the CCSD(T)/6-311+G(d,p)//BHandHLYP/6-311+G(d,p) level, four of the located channels may account for the hydrogen scrambling as they have overall barriers that are lower than the threshold of ~50 kcal/mol for hydrogen dissociation. Two lowest energy paths have been found. The first channel consists of skeletal rearrangement to the NCD radical cation (**3**) via a distonic isotoluene intermediate (**2**) followed by stepwise [1,5]-sigmatropic rearrangement (NCD walk). The second path involves a stepwise transfer of a methyl hydrogen atom to the *ortho*-position followed by interconversions of isotoluene radical cations by [1,2]-H shifts. The rate of both of these channels is predicted to be limited by the initial [1,2]-H shift from **1** to **2**, a step that requires a Gibbs activation energy of 38.7 kcal/mol. The third pathway involves skeletal rearrangement to the cycloheptatriene radical cation (**4**) via the mechanism proposed by Hoffman¹¹ (**1**–**2**–**3**–**4**) followed by [1,2]-H shifts in **4**. Indeed, the [1,2]-H shifts were previously predicted by MINDO/3 to be the most plausible mechanism for complete hydrogen scrambling in the system.¹³ However,

we have found that the TS for the [1,2]-H shift in **4** has a relative energy of 43.2 kcal/mol, which is higher than the barrier for the conversion of **1** to **2**. Finally, the fourth channel proceeds via concerted NCD walk with an overall barrier of 46.7 kcal/mol. As for the remaining located pathways, the Dewar–Landman mechanism, which transforms **1** to **4** via the methyl-encyclohexadiene radical cation (**5**), is found to proceed with much higher barriers as compared to those involved in the Hoffman mechanism. A novel rearrangement located in the present work, which connects **5** to **3** by concerted [1,2]-H shift and C–C bond formation, is also associated with a barrier much higher than that for hydrogen dissociation.

Acknowledgment. We thank the Swedish National Supercomputer Center (NSC) for generous allocation of computer time. We are very grateful to Prof. Olle Matsson for a valuable discussion.

Supporting Information Available: Absolute BHandHLYP SCF and CCSD(T) energies, BHandHLYP thermal corrections to Gibbs energy, and *xyz*-matrices of the BHandHLYP optimized stationary points. This material is available free of charge via the Internet at <http://pubs.acs.org>.

References and Notes

- (1) Lifshitz, C. *Acc. Chem. Res.* **1994**, *27*, 138.
- (2) Dunbar, C. D. *J. Am. Chem. Soc.* **1975**, *97*, 1382.
- (3) Ausloos, P. *J. Am. Chem. Soc.* **1982**, *104*, 5259.
- (4) Meyer, F.; Harrison, A. G. *J. Am. Chem. Soc.* **1964**, *86*, 4757.
- (5) Baer, T.; Morrow, J. C.; Shao, J. D.; Olesik, S. *J. Am. Chem. Soc.* **1988**, *110*, 5633.
- (6) Huang, F.-S.; Dunbar, R. C. *Int. J. Mass. Spectrom. Ion Processes* **1991**, *109*, 151.
- (7) Choe, J. C. *J. Phys. Chem. A* **2006**, *110*, 7655.
- (8) Rylander, P. N.; Meyerson, S.; Grubb, H. M. *J. Am. Chem. Soc.* **1957**, *79*, 842.
- (9) Baldwin, M. A.; McLafferty, F. W.; Jerina, D. M. *J. Am. Chem. Soc.* **1975**, *97*, 6169.
- (10) Howe, I.; McLafferty, F. W. *J. Am. Chem. Soc.* **1971**, *93*, 99, and references therein.
- (11) Hoffman, M. K. *Z. Naturforsch.* **1974**, *29a*, 1077, and references therein.
- (12) Kless, A.; Nendel, M.; Wilsey, S.; Houk, K. N. *J. Am. Chem. Soc.* **1999**, *121*, 4524, and references therein.
- (13) Dewar, M. J. S.; Landman, D. *J. Am. Chem. Soc.* **1977**, *99*, 2446.
- (14) Lifshitz, C.; Gotkis, Y.; Ioffe, A.; Laskin, J.; Shaik, S. *Int. J. Mass. Spectrom. Ion Processes* **1993**, *125*, R7.
- (15) Lias, S. G.; Bartmess, J. E.; Liebman, J. F.; Holmes, J. L.; Levin, R. D.; Mallard, W. G. *J. Phys. Chem. Ref. Data* **1988**, *17* (Suppl. 1).
- (16) Grützmacher, H.-F.; Harting, N. *Eur. J. Mass. Spectrom.* **2003**, *9*, 327.
- (17) Frisch, M. J.; Trucks, G. W.; Schlegel, H. B.; Scuseria, G. E.; Robb, M. A.; Cheeseman, J. R.; Montgomery, J. A., Jr.; Vreven, T.; Kudin, K. N.; Burant, J. C.; Millam, J. M.; Iyengar, S. S.; Tomasi, J.; Barone, V.; Mennucci, B.; Cossi, M.; Scalmani, G.; Rega, N.; Petersson, G. A.; Nakatsuji, H.; Hada, M.; Ehara, M.; Toyota, K.; Fukuda, R.; Hasegawa, J.; Ishida, M.; Nakajima, T.; Honda, Y.; Kitao, O.; Nakai, H.; Klene, M.; Li, X.; Knox, J. E.; Hratchian, H. P.; Cross, J. B.; Bakken, V.; Adamo, C.; Jaramillo, J.; Gomperts, R.; Stratmann, R. E.; Yazyev, O.; Austin, A. J.; Cammi, R.; Pomelli, C.; Ochterski, J. W.; Ayala, P. Y.; Morokuma, K.; Voth, G. A.; Salvador, P.; Dannenberg, J. J.; Zakrzewski, V. G.; Dapprich, S.; Daniels, A. D.; Strain, M. C.; Farkas, O.; Malick, D. K.; Rabuck, A. D.; Raghavachari, K.; Foresman, J. B.; Ortiz, J. V.; Cui, Q.; Baboul, A. G.; Clifford, S.; Cioslowski, J.; Stefanov, B. B.; Liu, G.; Liashenko, A.; Piskorz, P.; Komaromi, I.; Martin, R. L.; Fox, D. J.; Keith, T.; Al-Laham, M. A.; Peng, C. Y.; Nanayakkara, A.; Challacombe, M.; Gill, P. M. W.; Johnson, B.; Chen, W.; Wong, M. W.; Gonzalez, C.; Pople, J. A. *Gaussian 03, Revision C.02*; Gaussian, Inc.: Wallingford, CT, 2004.
- (18) Flükiger, P.; Lüthi, H. P.; Portmann, S.; Weber, J. *Molekul-4.3*; Swiss Center for Scientific Computing: Manno, Switzerland, 2000.
- (19) In fact, using a constrained optimization scan at the B3LYP/6-311+G(d,p) level of theory, we estimated the barrier for the methyl rotation in **1** to be 0.02 kcal/mol.
- (20) Feldman, V. I.; Sukhov, F.; Orlov, A.; Kadam, R.; Itagaki, Y.; Lund, A. *Phys. Chem. Chem. Phys.* **2000**, *2*, 29.
- (21) Symons, M. C. R.; Harris, L. *J. Chem. Res., Synop.* **1982**, 268.

(22) Fautitano, A.; Buttafava, A.; Martinotti, F. *Radiat. Phys. Chem.* **1995**, 45, 45.

(23) See, for example, Rogowska, A.; Kuhl, S.; Schneider, R.; Walcarius, A.; Champagne, B. *Phys. Chem. Chem. Phys.* **2007**, 9, 828.

(24) Norberg, D.; Larsson, P.-E.; Salhi-Benachenhou, N. *Org. Biomol. Chem.* **2006**, 4, 4241.

(25) Nguyen, M. T.; Landuyt, L.; Vanquickenborne, L. G. *Chem. Phys. Lett.* **1991**, 182, 225.

JP711166D